

Part IV - Ch 4 Waterways and water bodies

van Koningsveld, M.; van der Hout, A.J.; Vinke, Frederik R.S.; van der Werff, S.E.; de Vriend, H.J.

Publication date

2021

Document Version

Final published version

Published in

Ports and Waterways

Citation (APA)

van Koningsveld, M., van der Hout, A. J., Vinke, F. R. S., van der Werff, S. E., & de Vriend, H. J. (2021). Part IV - Ch 4 Waterways and water bodies. In M. V. Koningsveld, H. J. Verheij, P. Taneja, & H. J. de Vriend (Eds.), *Ports and Waterways: Navigating a changing world* (pp. 413-431). TU Delft OPEN Publishing.

Important note

To cite this publication, please use the final published version (if applicable).
Please check the document version above.

Copyright

Other than for strictly personal use, it is not permitted to download, forward or distribute the text or part of it, without the consent of the author(s) and/or copyright holder(s), unless the work is under an open content license such as Creative Commons.

Takedown policy

Please contact us and provide details if you believe this document breaches copyrights.
We will remove access to the work immediately and investigate your claim.

4 Waterways and port water areas

This chapter gives some examples of hydrodynamic phenomena and how these may affect water-borne transport systems.

4.1 Hydrodynamic effects on water-borne transport systems

The more supply chains aim at just-in-time delivery, the more they become vulnerable to workability limits and other hydrodynamic phenomena such as droughts. Operability is defined here as the capability to get work done under the conditions present and with the means available. It is the combination of these two attributes that determines operability, so not just the weather conditions, for instance. Even if the weather is fair, operability can be still restricted when water levels are reduced, or when a vessel, (un)loading or construction operation is particularly vulnerable to the ambient conditions.



Figure 4.1: Sea state, a determining factor of workability at sea (photo by RANJITH AR is free to use under www.pexels.com licence).

Various hydrodynamic phenomena can influence the operability of different parts of the supply chain:

- *Open ocean* – the main determining conditions here are wind, waves (Figure 4.1) and currents; vessels sailing at open sea have to exert extra power, hence more fuel and more emission, to maintain the **Speed Through Water (STW)**. Ocean currents may influence their absolute speed (**Speed Over Ground (SOG)**), which may increase or reduce the time and energy expenditure to a journey. Routing around severe currents may also lead to delays.
- *Offshore mooring and ports* – depending on the location (sheltered or not), offshore port-activities are much more sensitive, for example single buoy mooring, or barge transport in onshore-offshore port systems. Mooring forces must not become too large, vessel motions not too strong and offshore-onshore barge transport not unsafe.
- *Port entrance* – waves and currents (influencing manoeuvrability) and the shape and orientation of the entrance affect the potential for port downtime.

- *In-port manoeuvring* – depending on the amount of tug support available, vessel manoeuvring within a port may be hindered by strong cross-winds. In this case workability is determined by the occurrence of and exposure to high winds, as well as by the availability of tug support.
- *Moored vessels in a port* – have a resonant response to waves of certain frequencies, to the extent that the resulting motions may hamper loading/unloading operations and mooring forces may become unsafely large, forcing the vessel to leave the berth. Thus, operability is determined by the prevailing wave spectrum, the resonance properties of the port basin and the vessel, and the mooring system.
- *Moored vessels along a river* – are sensitive to strong currents, which may lead to overly large mooring forces. Hence operability is determined here by the occurrence of high flows, the degree of sheltering offered by the berth and the mooring system. Another potential cause of operability reduction is extremely low water, due to which the quay can no longer be reached (Figure 4.2), or sailing ships have to pass so close to the moored vessel, that vessel motions and mooring line forces become too large.



Figure 4.2: Tidal harbour of Lillo, province of Antwerp, Belgium, at low tide ([image](#) by LimoWreck is licenced under CC BY-SA 3.0).

- **IWT** – operability for vessels sailing on inland waterways can be influenced by various factors, such as high water (insufficient air draught under bridges), low water (insufficient navigable depth), blockage due to malfunctioning of infrastructure (bridge does not open, lock inaccessible), or blockage due to accidents.

Clearly, operability limits have their effect on the capacity of the supply chain, via delays or throughput reductions. Therefore, it may be worthwhile to invest into measures that increase operability.

[Stam \(2020\)](#) shows, in the case of an offshore-onshore container port system, how operability may influence the feasibility of a design option. The rapid increase in the amount of container transport, combined with the scarcity of available land onshore or the inability to receive still larger vessels, may force port authorities to seek extension offshore. This saves dredging costs, but involves double container handling and offshore-onshore transport, either by a barge shuttle service or via a fixed link (bridge, tunnel). A fixed link is expensive, while barge transport is subject to workability conditions. As a result, the economic feasibility of such a combined port system is not obvious.

Considering only two principal design parameters (design vessel size and distance offshore), [Stam \(2020\)](#) performs an economic feasibility study based on simulation for three different cases (Figure 4.3): (A) an onshore port including capital and maintenance dredging, (B) an onshore-offshore port combination with shuttle barges, subject to workability limits, and (C) an onshore-offshore port combination with a costly fixed link to the shore. The offshore port component includes a buffer stock in order to accommodate temporary mismatches between the throughput over the quay and the offshore-onshore transport system.

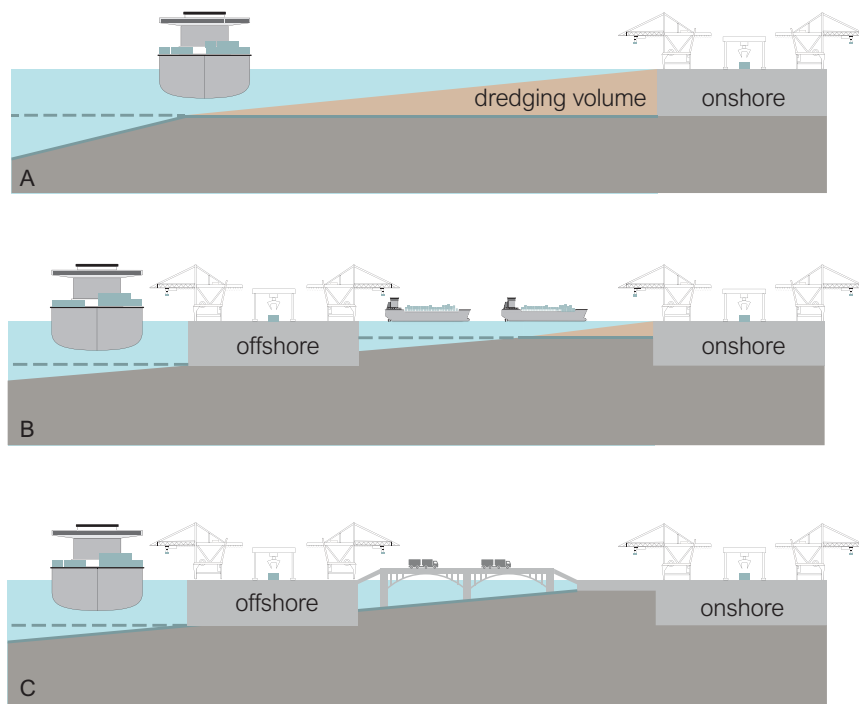


Figure 4.3: Case study of an offshore-onshore port system (reworked from [Stam, 2020](#), by TU Delft – Ports and Waterways is licenced under CC BY-NC-SA 4.0).

Referring to [Stam \(2020\)](#) for further details of the economic considerations, we focus here on the effect of operability on the costs of the system with a barge shuttle (Case B). Operability limits temporarily affect the capacity of the offshore-onshore system, hence the size of the buffer storage area offshore, which is an important cost item.

[Figure 4.4](#) gives, for the example considered, the relationship between the number of consecutive days of downtime (assumed to occur once per year) and the storage required if waiting times for the sea-going vessels remain within the agreed bounds.

In the example the yearly throughput via the offshore port is 500,000 **TEU**, which means on average 1370 **TEU** per day. The increase of the storage requirement per day of consecutive downtime, however, is significantly larger

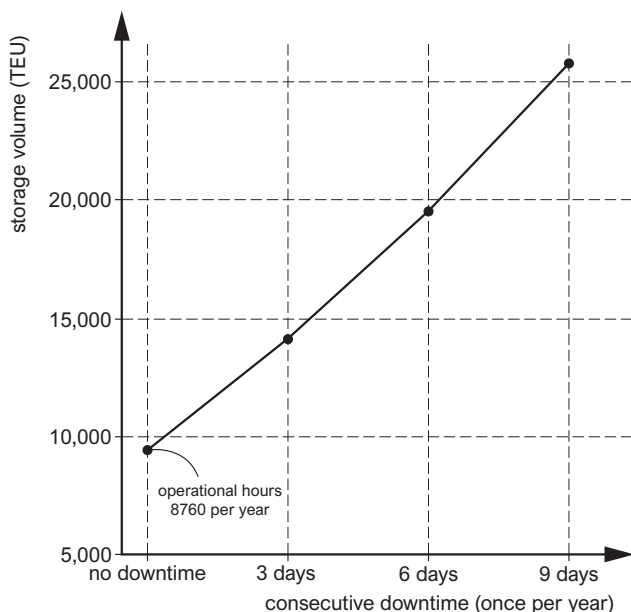


Figure 4.4: Storage volume requirement as a function of downtime (reworked from [Stam, 2020](#), by TU Delft – Ports and Waterways is licenced under CC BY-NC-SA 4.0).

(about 2000 TEU/day). This is due to the fact that vessels arrive at random (see [Part II – Chapter 4](#)). As the spare capacity of the shuttle barge system will generally not be large, it takes some time for the system to catch up after the downtime.

Apart from the costs of extra storage space, demurrage is another cost item. Demurrage is the charge paid to the shipping line for excess waiting time, above the agreed time. Daily demurrage rates typically range from 75 to 150 US\$/TEU. The optimal size of the storage area is largely the result of a trade-off between these cost items.

The left panel of [Figure 4.5](#) shows how in the example considered the downtime influences waiting costs and how this is reduced by increasing the offshore storage capacity. The relationship is nonlinear, because the storage capacity also determines the time needed after the downtime to return to normal. Subsequently, the investment costs involved in creating the storage capacity can be traded off against the capitalised waiting costs ([Figure 4.5](#), right) by seeking for the minimum sum of the two. Note, however, that waiting time is not only an economic issue but overly long waiting times also affect the port's reputation and its competitive edge.

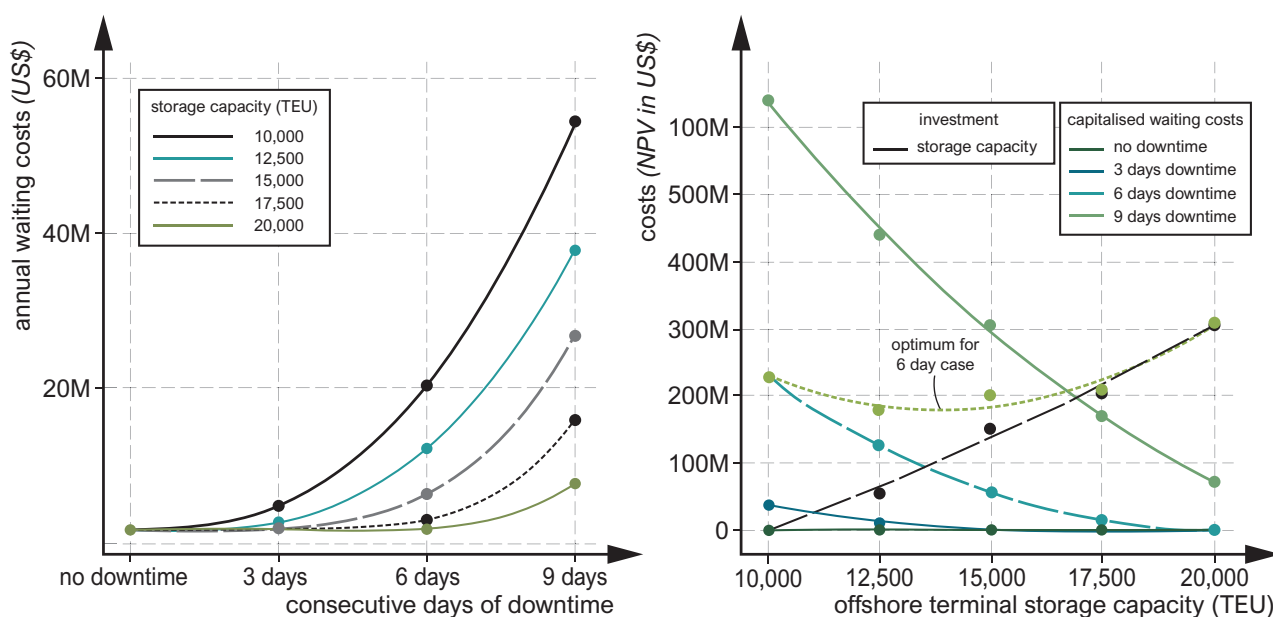


Figure 4.5: Downtime and optimum storage capacity (reworked from [Stam, 2020](#), by TU Delft – Ports and Waterways is licenced under CC BY-NC-SA 4.0).

The above example concerns a measure (buffer storage capacity) to accommodate downtime by reducing its effects. One may also consider measures to reduce the downtime, itself. Using the same categorisation as above, such measures could be as follows.

Open ocean Vessels sailing at open water are subject to wind, waves and currents. Wind and waves generally tend to reduce the [STW](#), which means more energy expenditure and emissions than in calm water. Routing ships around severe storms usually involves delays, which may mean delayed delivery to the client and the associated costs.

[Kim et al. \(2017\)](#) describe a method to estimate the loss of ship speed due to wind and waves. [Figure 4.6](#) shows some typical results, for an equivalent speed in calm water V_s of 23 knots. The left panel of [Figure 4.6](#) shows that wind and waves can cause significant speed reductions. Compensating this requires a disproportional extra energy consumption, which increases non-linearly as function of the speed ([Figure 4.7](#), left; also see [Chapter 5](#)). The right panel of [Figure 4.6](#) shows that even wind and waves astern don't add to the vessel speed.

Ocean currents, such as the Gulf Stream ([Figure 4.7](#), right), influence the [SOG](#) rather than the [STW](#). Their effect can be positive or negative, so clever routing can make the difference between costly delays and cost savings (due to slow steaming).

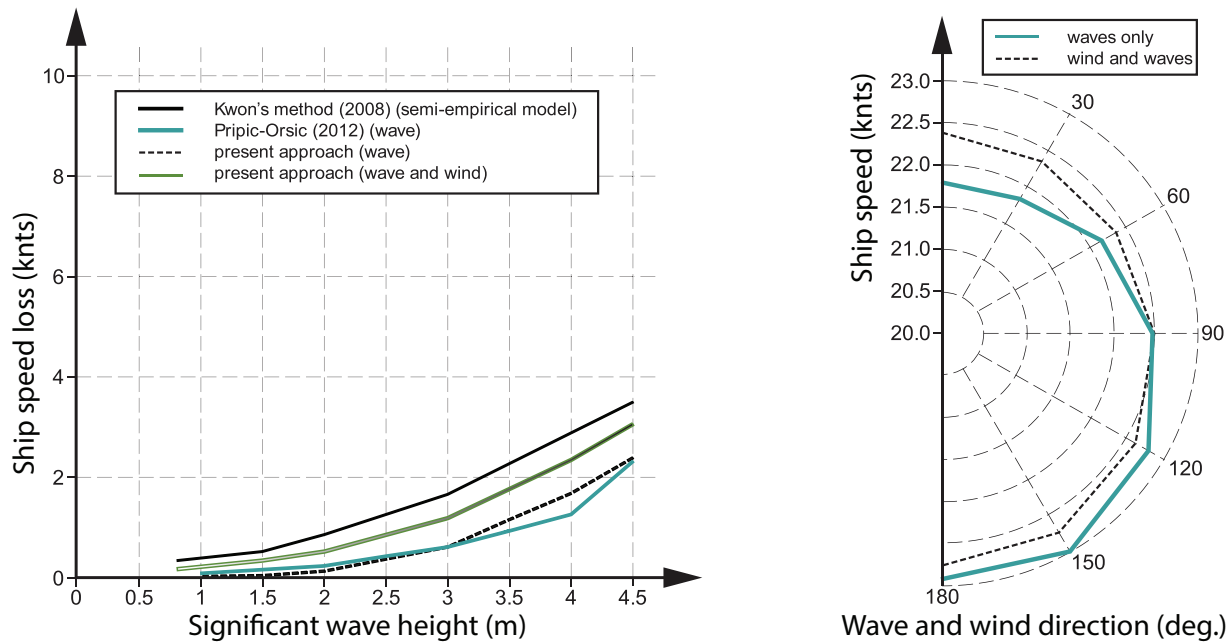


Figure 4.6: Vessel speed loss due to wind and waves at open sea (reworked from [Kim et al., 2017](#), by TU Delft – Ports and Waterways is licenced under CC BY-NC-SA 4.0). Left: speed loss with wind and waves ahead; right: dependence on wind and wave direction at wind force 6 Beaufort.

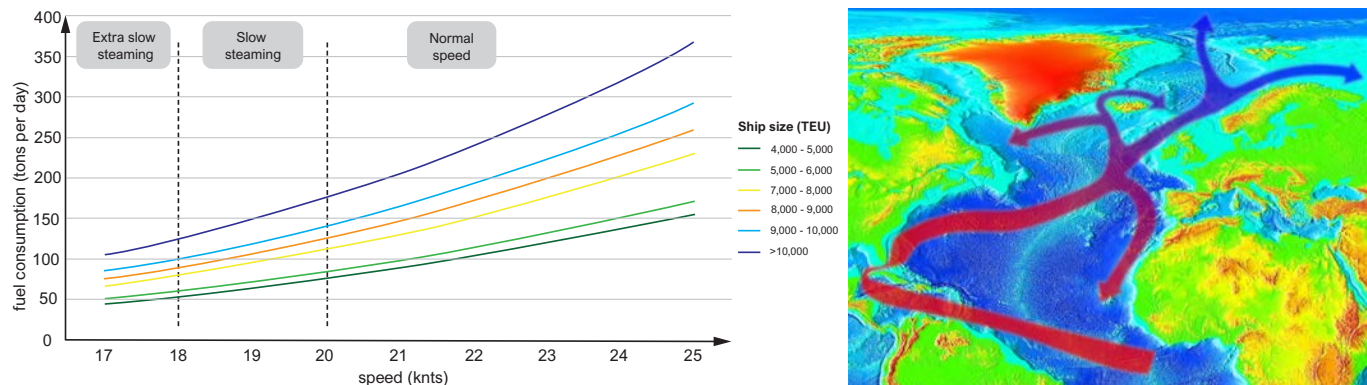


Figure 4.7: Left: Fuel consumption at open water (reworked from [Notteboom and Carriou, 2009](#), by TU Delft – Ports and Waterways is licenced under CC BY-NC-SA 4.0), right: Mid- and North-Atlantic currents (image by RedAndr is licenced under CC BY-SA 4.0).

Offshore moorings and ports Workability offshore can be enhanced by creating shelter from wind, waves and currents. If the existing topography is suitable (e.g. islands or sheltered bays) this can be achieved by clever location. Otherwise, structural measures are needed, e.g. an artificial port island. In the case of an onshore-offshore port system with shuttle barges, one may also consider alternatives in case of downtime of the barge system, such as a tidal window, or temporarily allowing smaller vessels only, or lightering (if downtimes occur often enough to justify the investment).

Port entrance A different breakwater layout may facilitate entering the port under harsh conditions. The possibility of increased wave penetration, however, is a point of attention. Further see [Part II – Section 3.2](#) and [Part III – Section 2.3](#)).

In-port manoeuvring Depending on the frequency of occurrence of troublesome high winds, the availability of extra tug assistance may be an option to increase workability. In the port layout design, the prevailing wind direction can be taken into account when determining the orientation of the quays.

Wind screens (Figure 4.8) are another possible structural measure. Note that the arguments to implement this type of measure are not only the reduction of downtime, but also the risk involved in manoeuvring. In the case of the Caland Canal, for instance, vessels have to take a sharp bend (not shown in Figure 4.8) just before passing the bridge. With unpredictable wind forces, this may involve a risk of material damage and downtime, but also of gas leakage, explosions and life hazard.



Figure 4.8: Wind screens along the Caland Canal, Port of Rotterdam (by Victor Stoeten is licensed under CC BY-NC-SA 4.0).

Moored in port Depending on the wave properties and the port layout, waves penetrating into a port may resonate there and increase in amplitude. A notorious example are seiches, which generally are hardly noticed at sea, but may become significantly larger inside the port and cause unacceptable ship motions there. It is difficult to prevent penetration of such long waves, but one may attempt to change the port's response properties, by a different layout, energy dissipating elements, etc. Dynamic mooring systems can help changing the combined response characteristics of the port and its mooring. Further see [Section 4.3](#).

Moored along a river An obvious measure to prevent unwanted current effects on vessels moored along a river is to create shelter from the current. In the design, however, one should keep in mind that shelter also tends to yield sedimentation.

Navigating inland waterways Downtime due to too high water levels on a river is difficult to avoid. This would require costly operations such as raising bridges. Moreover, sailing under these high flow conditions is not free from risk. The impact of blockage due to accidents or malfunctioning of infrastructure can be reduced by designating alternative routes beforehand (see [Part I – Chapter 2](#) for the example of the accident at the Grave weir). The effects of low water on water-borne supply chains are discussed in more detail in the next subsection.

4.1.1 Droughts and IWT supply chains

Especially in rain-fed rivers, droughts come with low river discharges. But also mixed-source rivers may exhibit times of low discharge. If the river is canalised, like the Maas, the water is retained behind weirs and navigability

is guaranteed, although the loss of water via the locks is a point of attention. In open rivers, like the Rhine downstream of Iffezheim in Germany, navigability is often guaranteed during a minimum number of days per year in an average year. In the case of the Rhine, this is defined by the discharge that is exceeded 95% of the time, the [Agreed Low Discharge \(ALD\)](#), at present $1020 \text{ m}^3/\text{s}$ at Lobith, near the Dutch-German border. Via model computations this is translated to an [Agreed Low Waterlevel \(ALW\)](#) at every point along the river. The bed of the navigation channel in the Waal and Lower Rhine, the main [IWT](#) fairway, is kept at 2.8 m below this level. The [IWT](#) system is tuned to this guaranteed navigable depth.

In times of drought, effects of low river discharges can to some extent be compensated by measures such as (also see [Ecorys, 2011](#)):

- reducing the load factor of the vessels,
- taking an alternative route with more navigable depth,
- using vessels with a smaller draught,
- a different operational concept, e.g. 24/7,
- shifting cargo to a different transport mode,
- temporary storage of cargo and stock depletion by the client,
- adaptation of production processes to defer the transport of raw materials,
- pro-active stockage.

In very dry years, the discharge falls below [ALD](#) for much longer than the agreed 5% of the time ([Kramer et al., 2019](#)). In 2018, for instance, this was almost four months in a row ([Figure 4.9](#)).

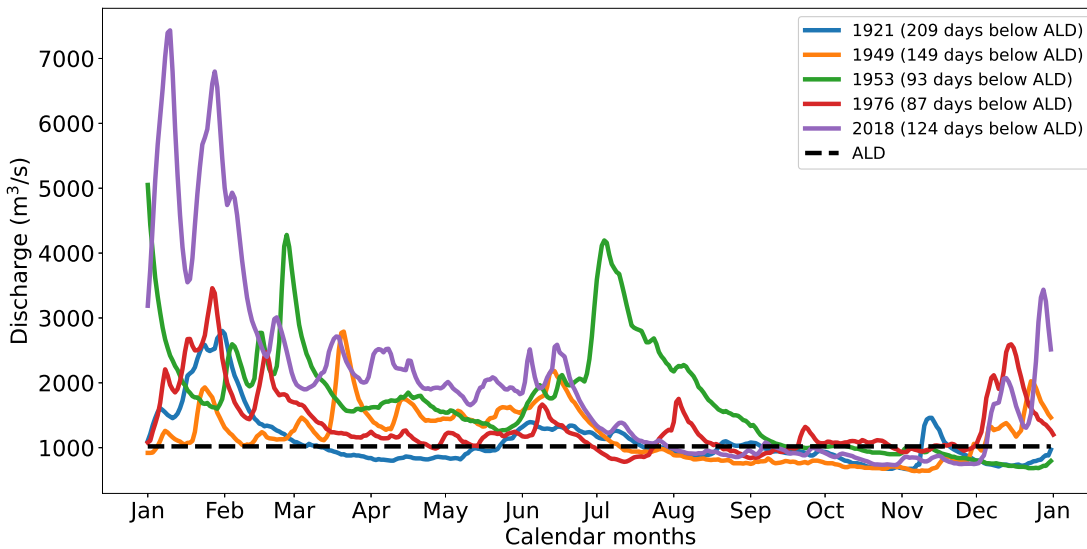


Figure 4.9: Rhine discharge at Lobith during a number of dry years (data provided by Rijkswaterstaat, image by TU Delft - Ports and Waterways is licenced under CC BY-NC-SA 4.0).

Clearly, this has its effects on [IWT](#), as [Figure 4.10](#) shows for dry bulk transport. Apart from the intuitive consequences of low water, viz. vessels adapting their cargo loads to reduce draught, which leads to an increased number of trips to transport the same amount of cargo, [Figure 4.10](#) clearly shows that as the river discharge changes, so does the fleet composition. [Vinke et al. \(2021\)](#) show that as soon as the discharge fell below [ALD](#), the larger push-barge convoys dropped out. The smaller ones could carry on somewhat longer, but ultimately had to give up, as well. The relatively small Rhine vessels remained unaffected and profited from the increased demand. The same applied, even more so, to the coupled barges. Yet, this increased activity of smaller vessels could not compensate entirely for the capacity loss, as the cumulative curve shows. This general picture of reduced transport performance, viz. more trips with less cargo per trip and less total capacity, is confirmed by data from Statistics Netherlands (CBS) from that same period, as shown in [Figure 4.11](#).

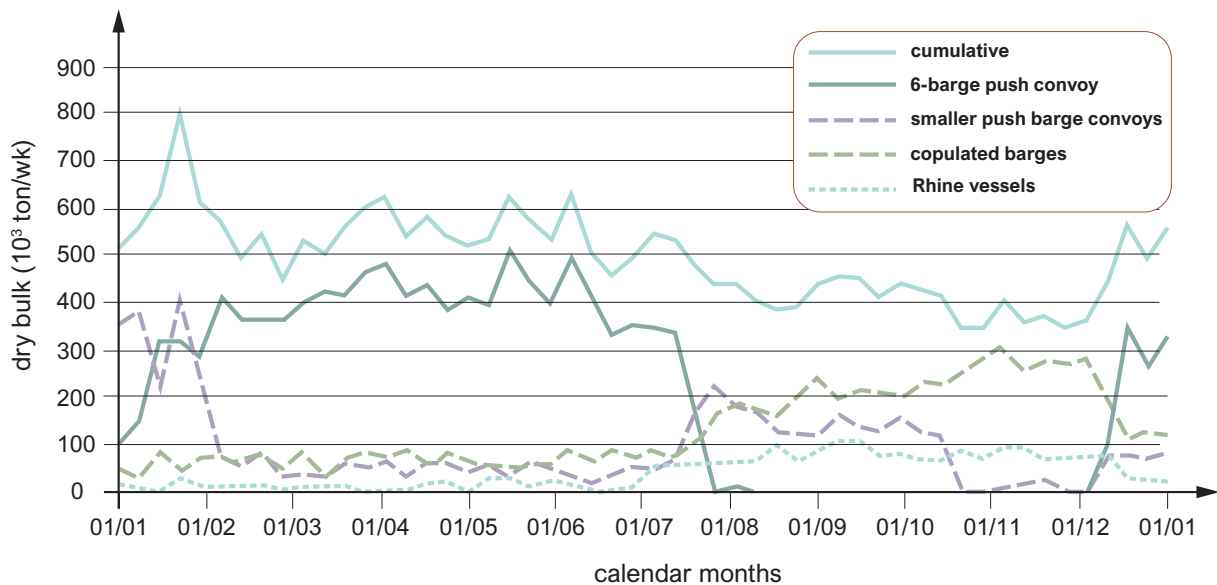


Figure 4.10: Response of dry bulk transport on the Rhine corridor to the 2018 drought (data provided by Rijkswaterstaat, image by TU Delft - Ports and Waterways is licenced under CC BY-NC-SA 4.0).

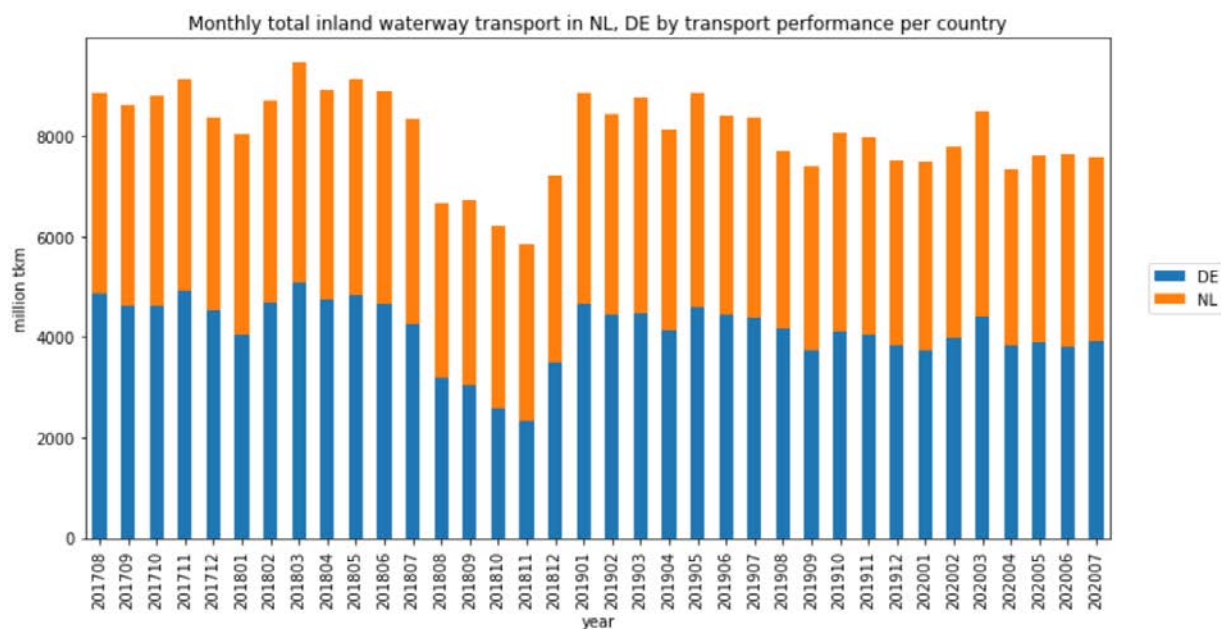


Figure 4.11: Influence of the 2018 drought on the total IWT transport performance in the Netherlands and Germany (data provided by CBS, image by TU Delft - Ports and Waterways is licenced under CC BY-NC-SA 4.0).

Apart from carrying less cargo, the vessels also sail slower, because they are loaded up to the maximum allowable draught. As a consequence, they experience on average more resistance while sailing. So, it takes not only more trips to transport the same amount of cargo, but it also takes longer per trip, even if there is no hindrance from other vessels. Moreover, the larger number of vessels leads to a higher traffic intensity, hence a reduced capacity of the waterway (see Section 2.2.2). Vinke et al. (2021) showed with an agent-based simulation model (OpenCLSim) that depth bottlenecks way up in the hinterland, triggered an increase in IWT port calls in the Port of Rotterdam, a phenomenon that can also be observed in Automatic Identification System (AIS) data of that period. This increased traffic intensity in turn contributed to port congestion and delays.

Yet, changes in fleet composition, an increased numbers of trips and extra resistance are not the only cause of delays during droughts. Especially in rivers, the navigable width also decreases (Figure 4.12). This means that vessels have less space for manoeuvres such as overtaking. Hence the risk of accidents or grounding incidents increases, the more so because the traffic intensity increases. This explains why during the 2018 drought Rijkswaterstaat issued a ban on overtaking for various parts of the Dutch waterway network. As a consequence, traffic congestion occurred at various bottlenecks in the system. The right panel of Figure 4.12 shows that the mean navigable width is equal to the guaranteed 200 m at ALD (1020 m³/s at Lobith), but decreases significantly at lower discharges, down to 123 m at 600 m³/s. At bottlenecks, the decrease is even stronger, to less than a third of the width at ALD. Based on traffic simulations with SIMDAS, Verschuren (2020) shows that in this part of the river the width reduction had a stronger effect on the delays than the depth reduction or the increased traffic intensity.

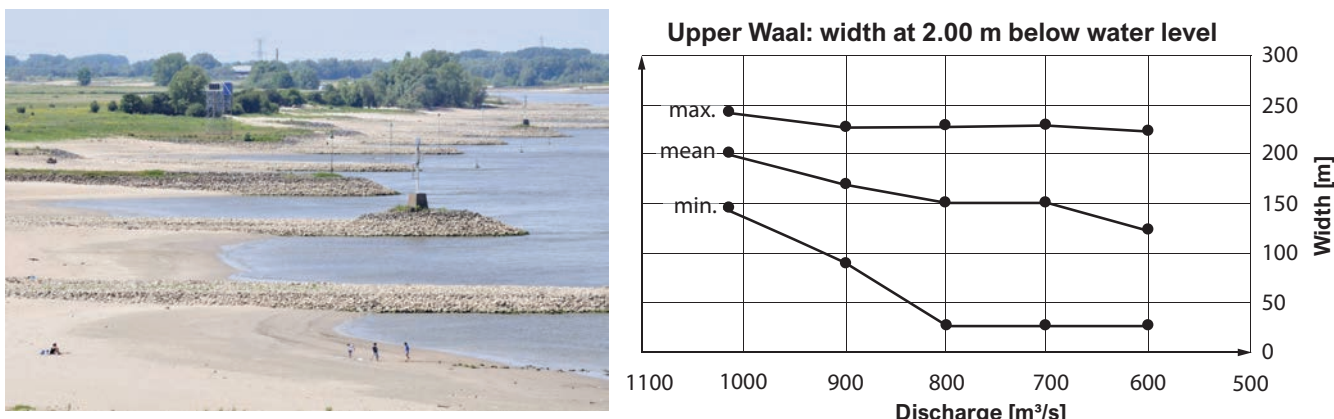


Figure 4.12: Reduced navigable width at low water (left: beeldbank.rws.nl, Rijkswaterstaat, by Martin van Lokven; right: reworked from Verschuren (2020) by TU Delft – Ports and Waterways is licenced under CC BY-NC-SA 4.0).

These consequences of low discharge extremes on the IWT transport mode, clearly underline that ports and waterways should be viewed as integral parts of a coherent system. The complex interplay between water motion, state of the infrastructure, vessel behaviour and logistics needs to be understood fully in order to understand what is happening and to enable the rational design of mitigating measures. The next sections discuss some other examples of hydrodynamic effects on supply chains.

4.2 Hydrodynamic effects during locking

In Part III we have discussed the hydrodynamic phenomena during locking, but did not focus on the forces exerted on the vessels during the locking process and the consequences for locking times and mooring forces.

4.2.1 Entering the lock

When a vessel enters a lock, it experiences a more or less sudden reduction of the cross-sectional area. As a consequence, the return flow and the water level draw-down suddenly increase. On the one hand, this enhances the resistance the vessel encounters; on the other hand it sends a translatory wave into the lock chamber, and a smaller one into the approach channel.

The wave in the lock chamber bounces against the closed gate, comes back and hits the vessel, thus causing even more resistance (Figure 4.13). These effects will obviously be stronger as the blockage factor increases. The right panel of Figure 4.13 clearly illustrates this: the velocity reduction of a small motor ship (dash-dotted line) is much less than that of the pushed convoys.

Measurements in a physical scale model of the new sea lock at IJmuiden give more quantitative information. Figure 4.14 shows the experimental set-up, Figure 4.15 the principal results.

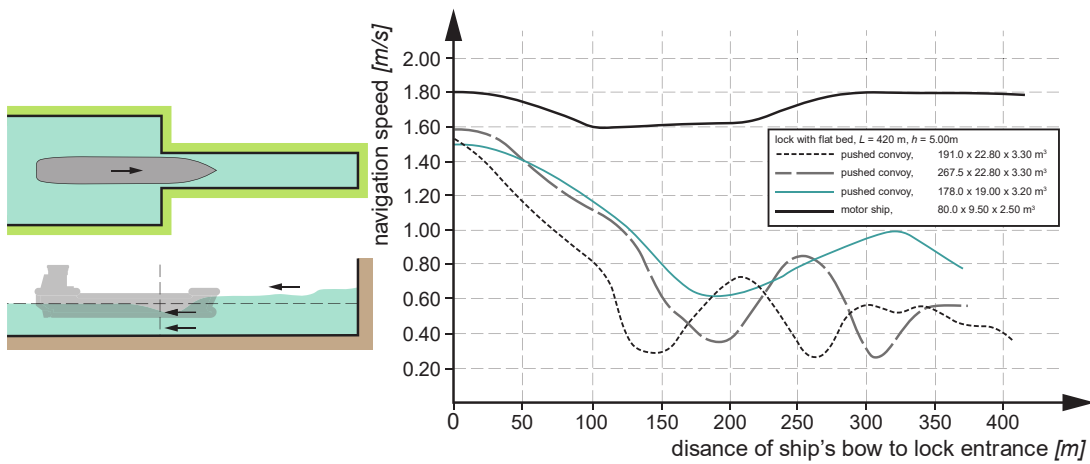


Figure 4.13: Hydrodynamic phenomena during lock entrance (by TU Delft – Ports and Waterways is licenced under CC BY-NC-SA 4.0).

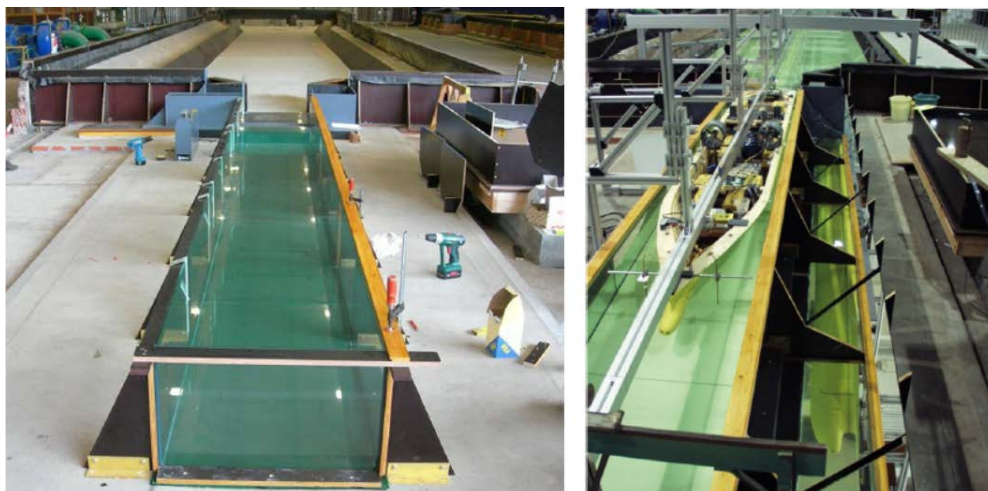


Figure 4.14: Overview of the physical scale model of the new IJmuiden sea lock (source: Deltares).

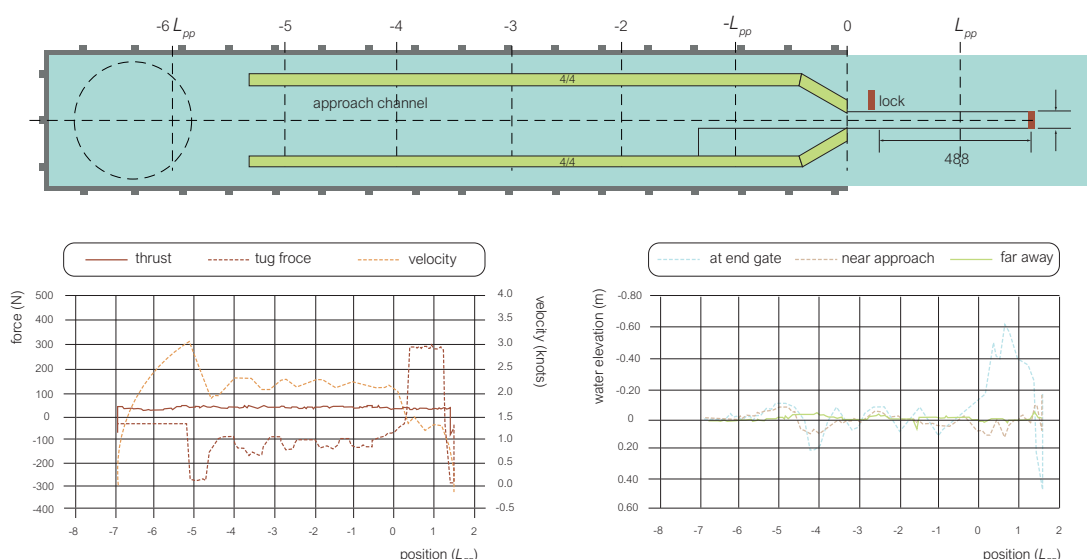


Figure 4.15: Example of experimental results from the IJmuiden scale model (source: Deltares). Image by TU Delft – Ports and Waterways is licenced under CC BY-NC-SA 4.0.

When the translatory wave bounces against the closed gate (Figure 4.16), it exerts a pressure force that may damage the gate. This force is a function of the maximum wave height z_{max} at the gate, hence of the vessel speed and the blockage factor:

$$\frac{z_{max}}{h_0} = 1.44 \frac{V_s^2}{gh_0} \frac{A_s/A_{lock}}{1 - A_s/A_{lock}} \quad (4.1)$$

in which the coefficient has been determined empirically. The length of the vessel turns out to be less important.

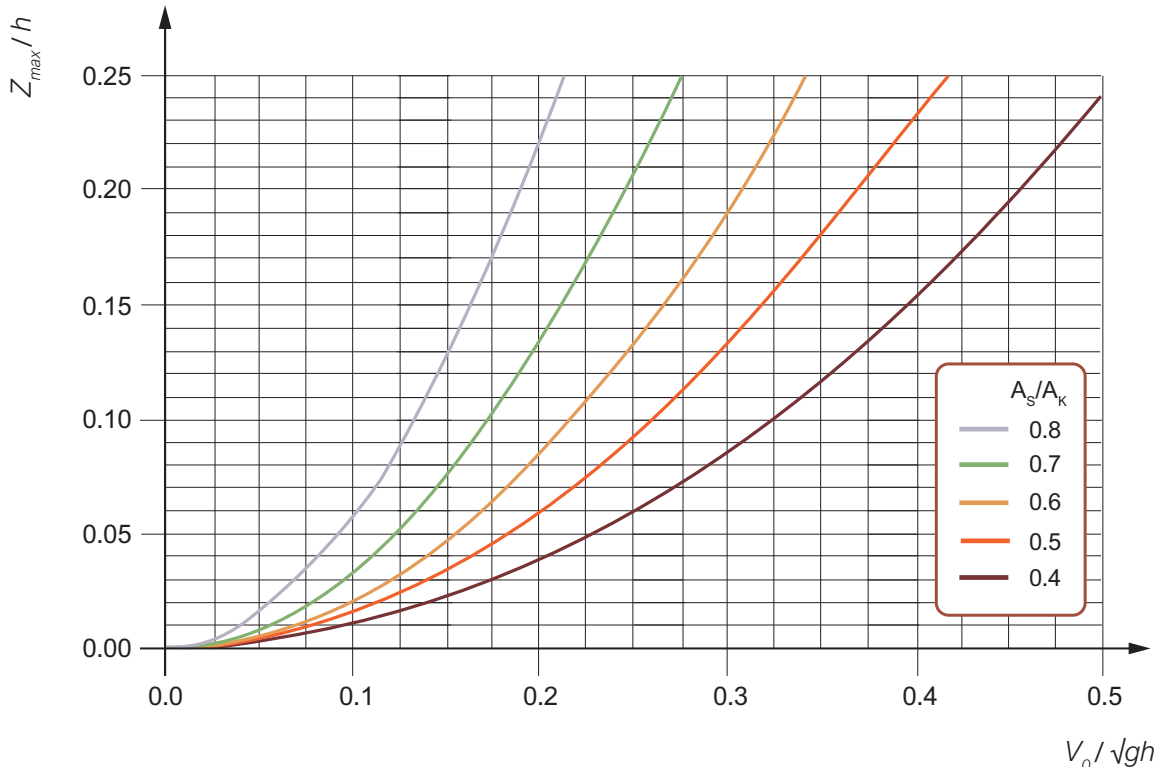


Figure 4.16: Maximum height of the translatory wave at the closed gate (image by TU Delft - Ports and Waterways is licenced under CC BY-NC-SA 4.0).

In order to prevent damage to the gate, the vessel entrance speed is restricted. Another reason to do so is that other vessels that are already in the lock chamber will experience the effect of the translatory wave, in the form of ship motions and/or mooring line forces. As the allowable forces on a vessel or its mooring lines are expressed as a percentage of the vessel's water displacement, the speed restriction will be more severe if there are small vessels in the lock chamber. This may even influence the lock capacity.

Lock entrance can also be simulated with a **Computational Fluid Dynamics (CFD)** model. Though quite computationally demanding, such a model is able to capture the physics of hydrodynamic phenomena during locking operations. This includes viscous effects, which become important in very confined areas, e.g. at large values of the blockage factor. Figure 4.17 gives a typical result of such a model.

4.2.2 Forces when filling the lock chamber

There are various options to fill a lock chamber, e.g.

- by opening valves in the lock gates,
- by opening culverts in the chamber walls,
- by lifting or tilting the end gate.

In Part III - Chapter 4 we have described how the water level in the chamber responds to the opening procedure. Here we will consider the forces exerted on a vessel in the chamber. In order to prevent overloading or even

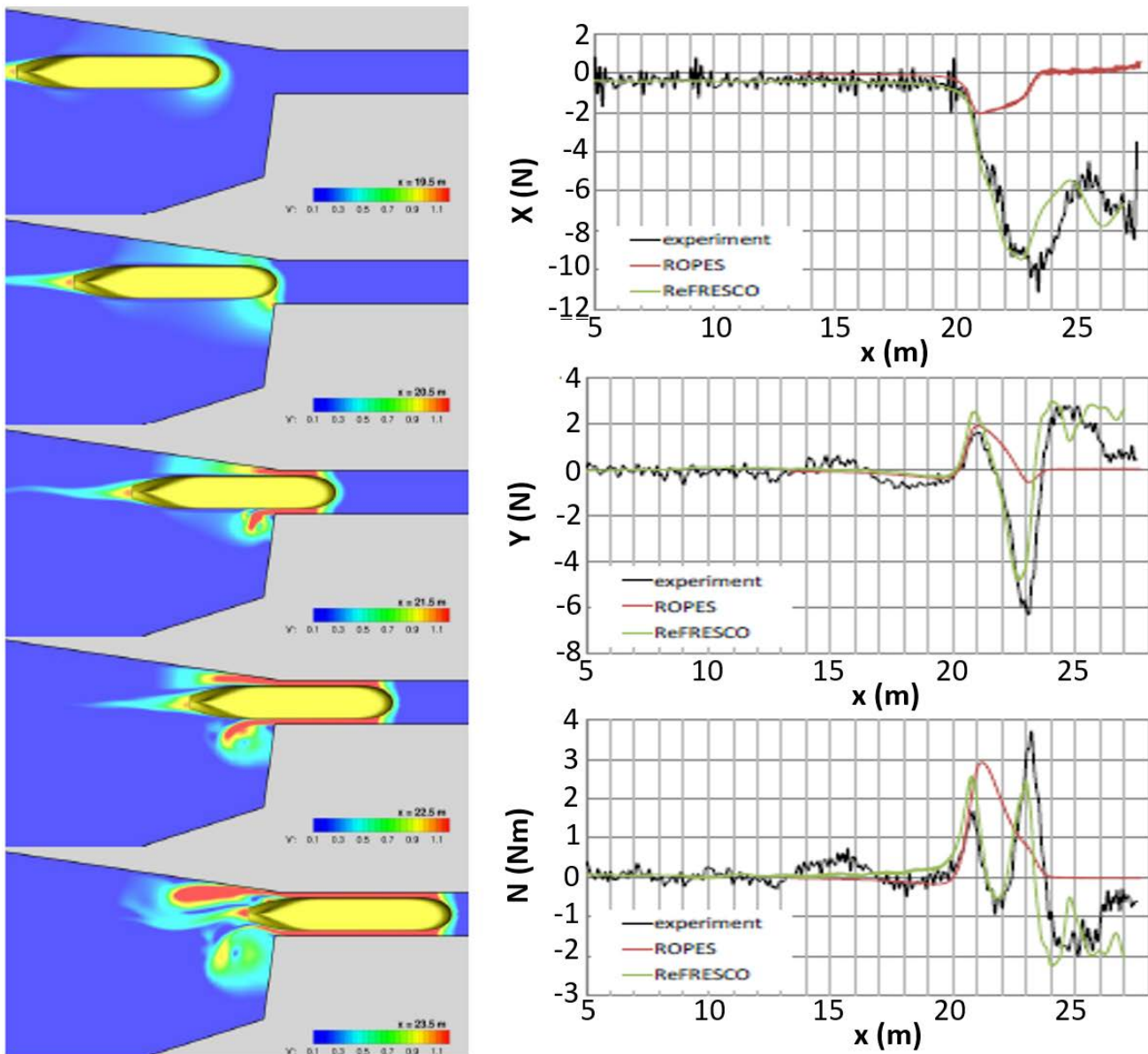


Figure 4.17: Numerical model results for a ship entering a lock ([Toxopeus and Bhawsinka, 2016](#)); left: velocity fields; right: longitudinal and transverse forces and moment exerted on the vessel. Images are licensed under CC BY 4.0.

snapping of mooring lines (a dangerous event especially for people on the lock platform), these forces are limited. Such limitations are expressed as a permillage of the vessel's weight (water displacement). [Table 4.1](#) gives the numbers for some [IWT](#) vessel classes.

Vessel class	Maximum mooring line forces (% of water displacement)	
	during filling	during emptying
CEMT Class III	1.50	2.00
CEMT Class IV	1.10	1.50
CEMT Class Va	0.85	1.15

[Table 4.1: Maximum mooring line forces during lock chamber filling or emptying \(by TU Delft – Ports and Waterways is licenced under CC BY-NC-SA 4.0\).](#)

The forces exerted on a vessel during filling consist of various components. [Figure 4.18](#) summarises them for the case of filling through the end gate. Note the importance of water level gradients inside the chamber.

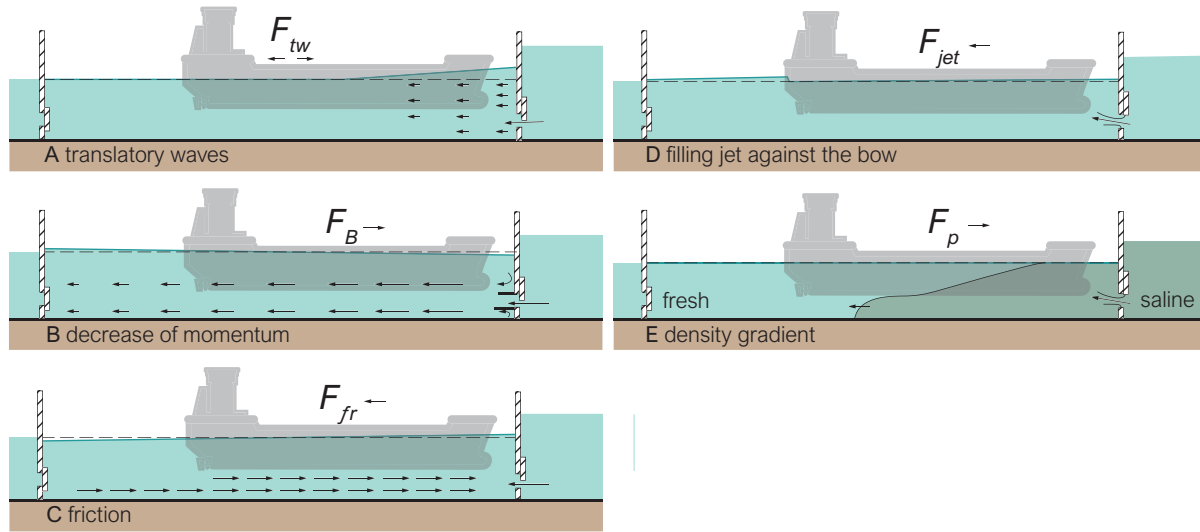


Figure 4.18: Forces exerted on a ship during lock filling (reworked from [Glerum and Vrijburcht, 2000](#), by TU Delft – Ports and Waterways is licenced under CC BY-NC-SA 4.0).

The force due to a translatory wave, for instance, can be evaluated as follows (also see [Figure 4.19](#)):

$$F_{tw} = B_s \left[\frac{1}{2} \rho_w g (z + D_s)^2 - \frac{1}{2} \rho_w g D_s^2 \right] = \rho_w g B_s \left(z D_s + \frac{1}{2} z^2 \right) \quad (4.2)$$

When ignoring the (small) quadratic term, this becomes:

$$F_{tw} = \rho_w g B_s L_s D_s \frac{z}{L_s} = \text{water displacement} \times \text{water level slope over the ship} \quad (4.3)$$

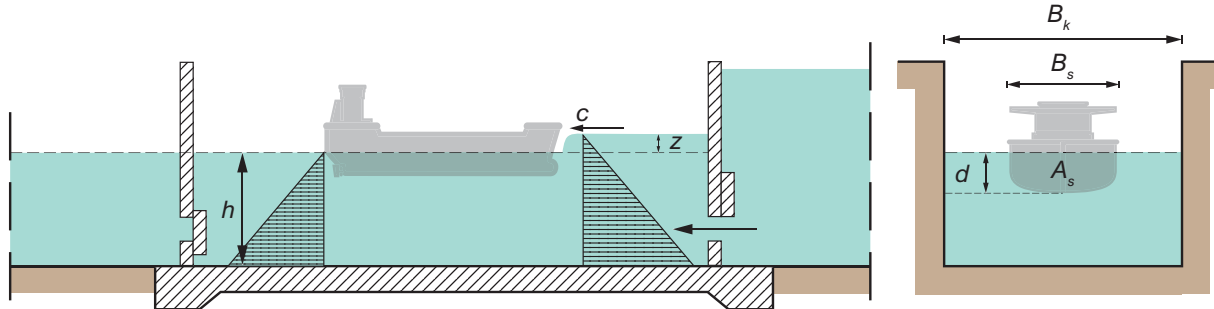


Figure 4.19: Force exerted on a ship by a translatory wave (by TU Delft – Ports and Waterways is licenced under CC BY-NC-SA 4.0).

The contribution of the jet force can be taken into account by adding the difference in momentum flux at the bow and the stern, respectively ([Van Loon, 2017](#)):

$$F_{ship} = S_b + \frac{1}{2} \rho_w g h_b^2 - \rho_w \frac{Q^2}{A_{lock,s}} - \frac{1}{2} \rho_w g h_s^2 \quad (4.4)$$

in which the suffix b refers to the bow and the suffix s to the stern of the ship. Furthermore, S_b is the momentum flux of the jet hitting the bow of the ship, Q the jet discharge and $A_{lock,s}$ the cross-sectional area of the lock chamber just behind the stern. [Figure 4.20](#) presents results from laboratory measurements, showing how the jet force depends on the under keel clearance and the distance of the ship from the gate ($x_{b,min}$ is the minimum allowable distance of the bow from the gate). Note that for large **Under Keel Clearance (UKC)** values the force can become negative, due to the head difference between bow and stern. Also note that the dependence on the distance to the gate is non-trivial.

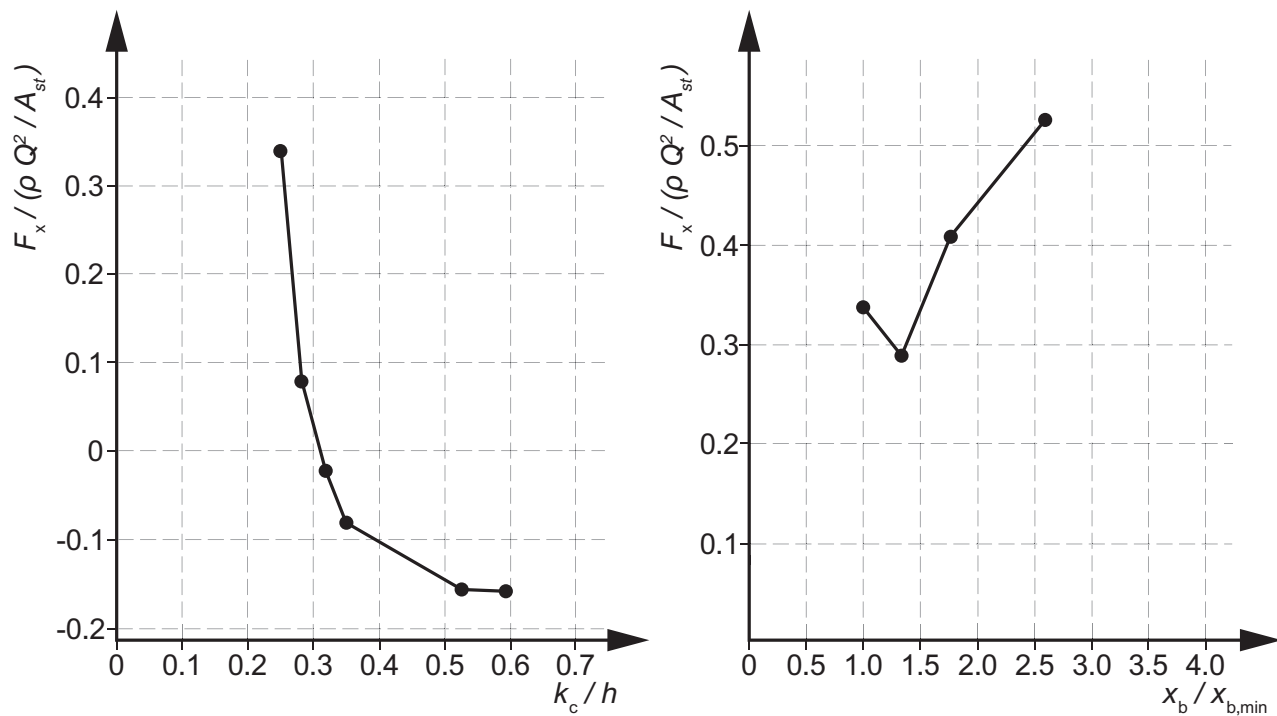


Figure 4.20: Jet force dependence on under keel clearance and distance from the gate (reworked from [Van Loon, 2017](#), by TU Delft – Ports and Waterways is licenced under CC BY-NC-SA 4.0).

The forces exerted on a ship during locking can also be determined with a physical scale model, or with a numerical model. Figure 4.21 shows an example from a scale model of a lock with a large bulk container. The results clearly show the effect of the translatory waves during filling, as well as the disturbance that remains after the chamber has been filled.

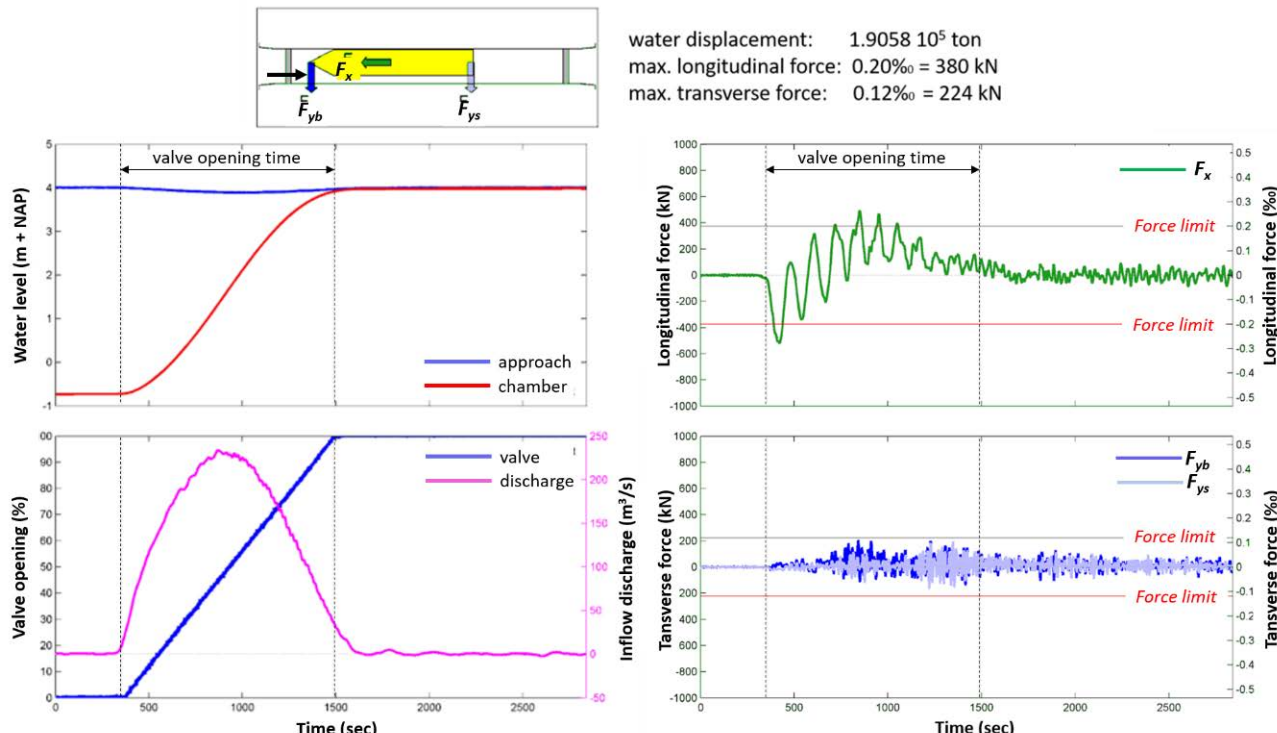


Figure 4.21: Forces exerted on a ship during lock filling (scale model experiment) (source: Deltaires).

4.2.3 Forces when emptying the lock chamber

When the lock chamber is emptied, the ship is exposed to forces, again, though with less constituents (Figure 4.22). The effects of the filling jet and the density gradient are missing now, the former because the jet is directed out of the chamber now, the latter because there is no water with a different density entering the lock.

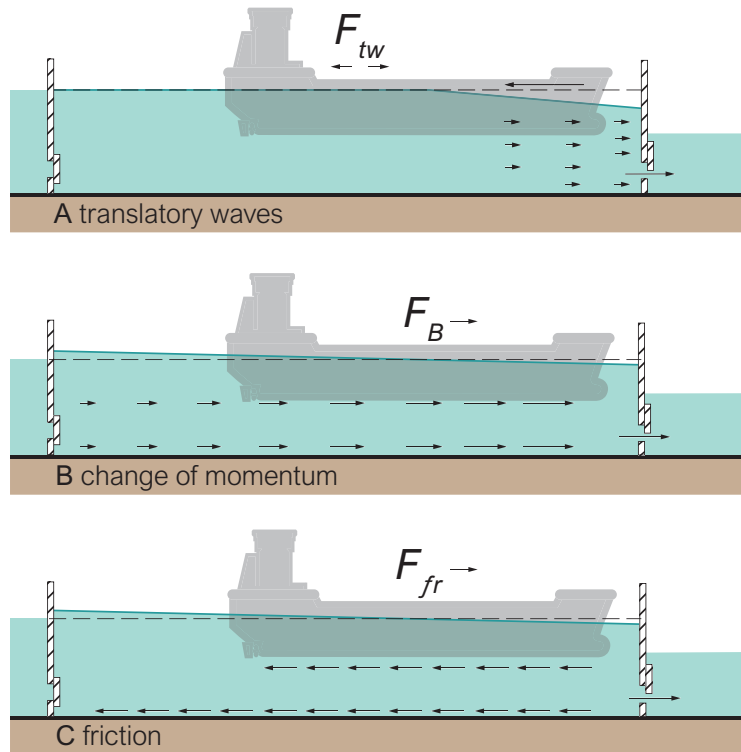


Figure 4.22: Forces on a ship during lock emptying (reworked from [Glerum and Vrijburcht, 2000](#), by TU Delft – Ports and Waterways is licenced under CC BY-NC-SA 4.0).

4.2.4 Exiting the lock

During lock exit, the vessel first passes the narrow lock section, where it creates a water level set-down and a return current. Depending on the blockage ratio, it also pushes water out of the lock, thus sending a negative translation wave into the lock and a lower positive one into the downstream channel (Figure 4.23).

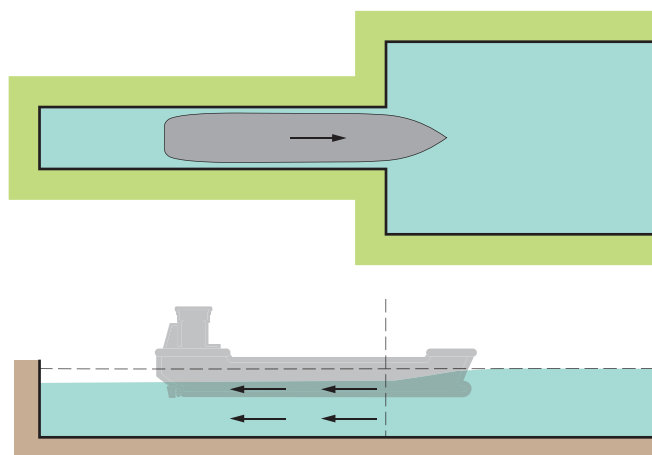


Figure 4.23: Hydrodynamic phenomena during lock exit (reworked from [Glerum and Vrijburcht, 2000](#), by TU Delft – Ports and Waterways is licenced under CC BY-NC-SA 4.0).

Experiments in a scale model of the new locks of the Panama Canal (Vantorre et al., 2012) give an impression of the forces exerted on a ship, in this case a large container carrier (12,000 TEU, 265 x 46 x 15.2 m), when it leaves the lock (Figure 4.24). Note that when the stern leaves the lock (bow position at L_{pp}) the vessel undergoes a strong positive force and the tugs have to exert an opposite force in order to keep it at the desired speed.

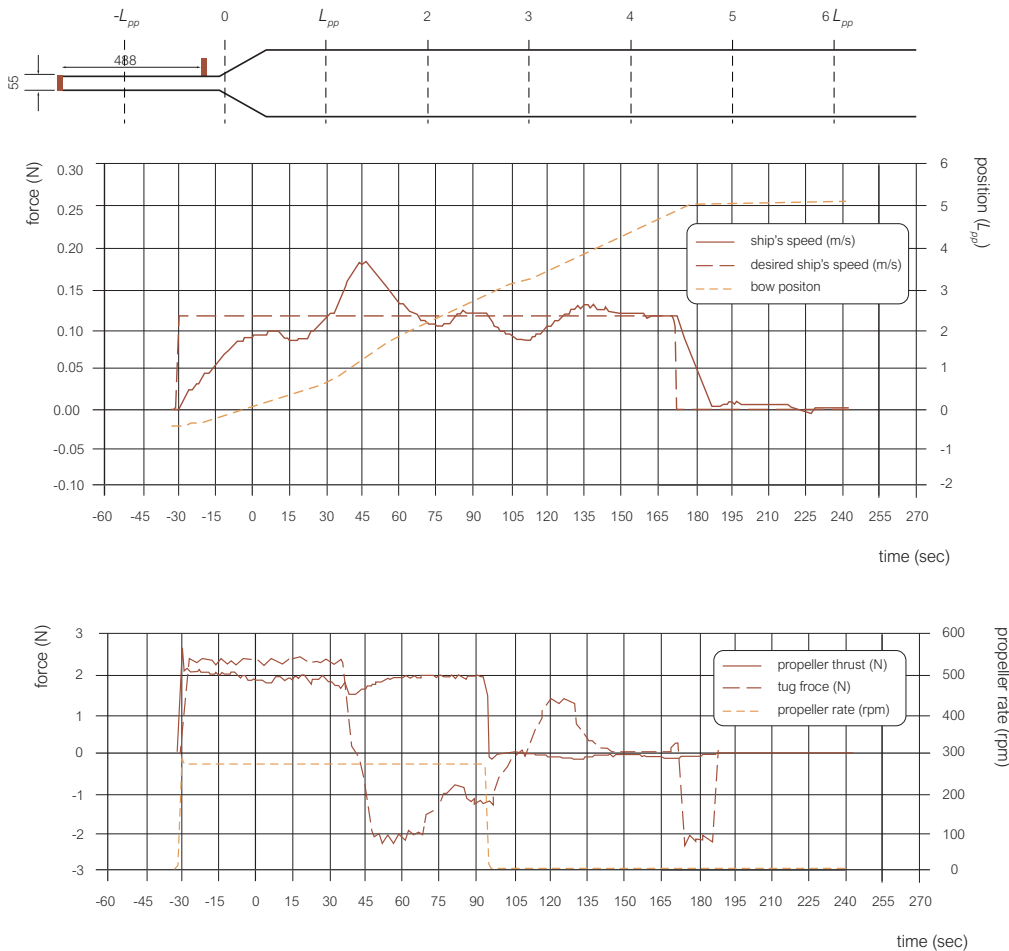


Figure 4.24: Forces exerted on a ship that leaves a lock (reworked from Vantorre et al., 2012, by TU Delft – Ports and Waterways is licenced under CC BY-NC-SA 4.0).

4.3 Hydrodynamic effects on moored vessels

Loading and offloading operations may require an evaluation of the hydrodynamic loads if there are safety risks (of snapping lines or even vessels breaking free) or the risk of downtime (reduced cargo handling capacity). In general, moored vessels move due to wind and long (infra-gravity) waves. Additionally, vessels moored in harbours may experience effects of passing vessels, and vessels moored at exposed terminals also encounter sea and swell waves, and possibly currents.

A **Dynamic Mooring Analysis (DMA)** is executed to evaluate the motions of moored vessels and the loads in the mooring lines. This is done based on information about the environmental conditions, vessel characteristics and mooring configuration.

4.3.1 Analysis input

Environmental conditions that are considered in the analysis are combinations of wind, current, and sea/swell waves or waves due to passing ships. A wave spectrum represents a particular wave condition at a certain location by a superposition of regular wave components. The frequencies of these wave components are given on the

horizontal axis and their energy density is given on the vertical axis. Part II – Figure 2.24 shows all relevant wave types and their frequency ranges.

The vessel characteristics required for the mooring analysis are related to calculating the forces and moments on the vessel due to wind, current and waves. For wind and current, coefficients and areas are used to determine the forces and moments on the vessel due to a wind/current of a certain speed and certain direction with respect to the vessel. For waves, a database of **Response Amplitude Operators (RAOs)** is required. This indicates the response amplitude of the vessel to a wave component with an amplitude of 1 m, for the entire range of wave frequencies, for the entire range of relative wave directions, and for all six degrees of freedom.

Figure 4.25 (left) shows the response spectrum of a tanker in beam seas for the heave motion. It can be seen that for long waves (small frequencies) the RAO is about 1, indicating that the response amplitude is equal to the wave amplitude. The vessel simply slowly moves up and down along with the incoming wave. Towards a frequency of 0.5 rad/s (12.5 s), the RAO increases to 1.6, indicating the natural frequency for heave. For very short waves, the vessel does not move at all. Figure 4.25 (middle) shows the response spectrum of the tanker for pitch in head waves. The natural frequency is at about 0.6 rad/s. The large peak at 0.4 rad/s indicates the wave length, that is approximately equal to the vessel length. Thus, by looking at the response spectra of the vessel and comparing these to the wave spectrum, an estimate can be made of which wave frequencies might cause (extreme) motions of the vessel.

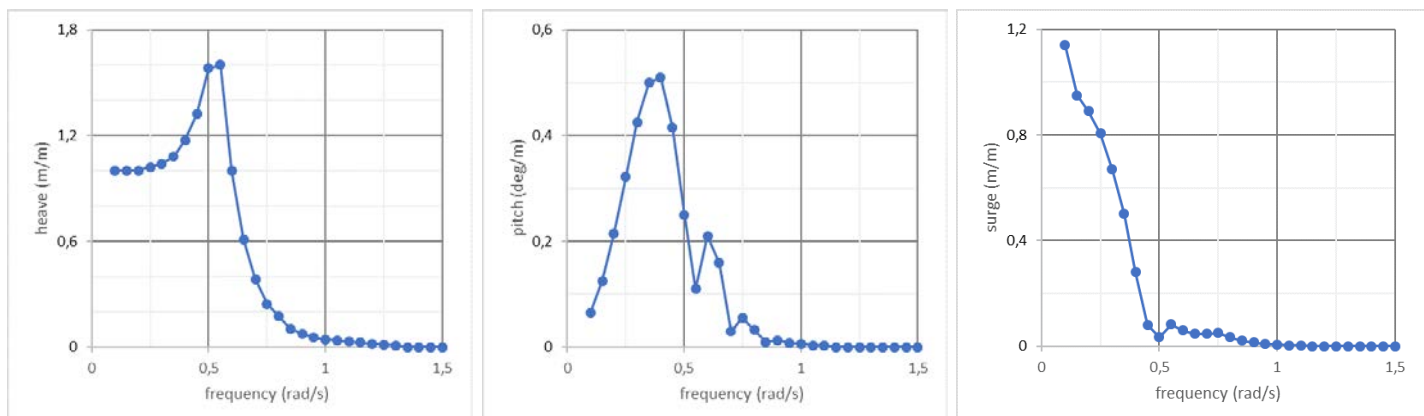


Figure 4.25: Typical RAOs for a tanker shaped vessel (left: heave motion in beam seas; middle: pitch motion in head seas; right: surge motion in head waves). Images by TU Delft – Ports and Waterways are licenced under CC BY-NC-SA 4.0.

As a final input, the mooring configuration is required. This includes the mooring line properties (length, elasticity), fenders and possibly tools for dampening the vessel motions (see Figure 4.26).

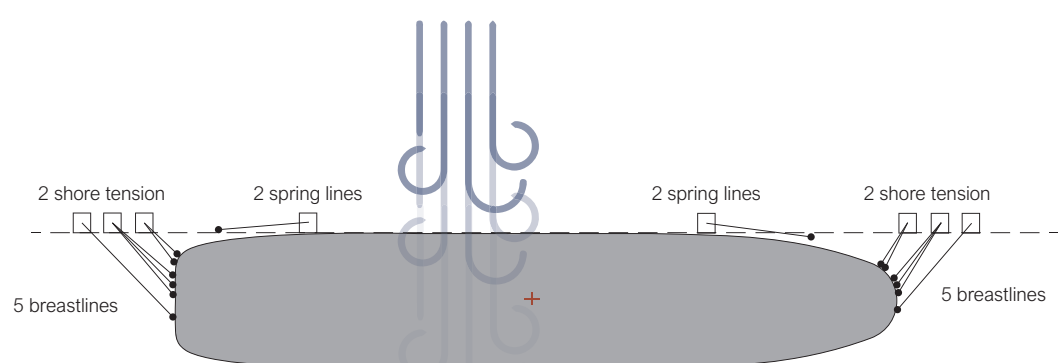


Figure 4.26: An example of a mooring layout (by TU Delft – Ports and Waterways is licenced under CC BY-NC-SA 4.0).

4.3.2 Time domain simulation

Based on the input, a simulation is conducted to obtain the vessel motions and forces in the mooring lines. This simulation is done in time domain, so all information captured in the frequency domain is translated to the time domain. One simulation is executed for each combination of input parameters.

Often, a large number of environmental conditions is evaluated, ranging from day-to-day conditions to extreme conditions. To assess which layout of mooring lines, fenders and damping tools allows for the highest uptime and smallest safety risk, multiple mooring configurations are evaluated. On top of that, multiple vessel draughts may need to be evaluated, resulting in the assessment of several vessel databases and coefficients. As a result, the number of simulations to be executed increases rapidly.

After post-processing and analysing all simulation results, the (extreme) vessel motions and (extreme) mooring forces are reported. A comparison of the performance of the various mooring configurations is then made. Based on this, recommendations can be made for the best mooring configuration to use, and the effectiveness of additional damping tools.

4.3.3 Dampening measures

In case it is found in the [DMA](#) that a conventional mooring configuration has a high risk of downtime or even safety issues, additional measures are considered. As can be seen in [Figure 4.25](#) (right), the surge motion of a vessel is sensitive to low frequent excitations. Examples of low frequent excitations are wind, long period waves and passing vessels; all typical effects that are encountered by a moored vessel. As a result, the moored vessel may start to move excessively in surge direction.

ShoreTension is a system designed by the Royal Boatmen Association Eendracht (KRVE) to dampen the horizontal vessel motions in the frequency range around the natural frequency of the system. The system absorbs vessel motion energy by adding a cylinder to the mooring lines that pays out and heaves in line length, ensuring a constant line tension.

[Figure 4.27](#) indicates the effect of the ShoreTension system on a moored heavy transport vessel. The blue graph indicates the spectral density for the vessel with original mooring configuration, and the purple graph indicates that of the same vessel with the ShoreTension system as part of the mooring configuration. For the surge motion ([Figure 4.27](#), top), the ShoreTension system is capable of significantly reducing the slowly varying horizontal motions (around the natural frequency of the system of 0.15 rad/s). There is however another peak present for this moored vessel configuration, between 0.4 and 0.5 rad/s. These motions could be excited by ordinary gravity waves (as defined in [Part II – Figure 2.24](#)). The motions in this frequency range are not affected by the presence of ShoreTension. In the bottom figure of [Figure 4.27](#), it can be seen that the natural frequencies for the sway motion are different than for surge, and that the ShoreTension system has a different (reduced) effect on the reduction of the motions.

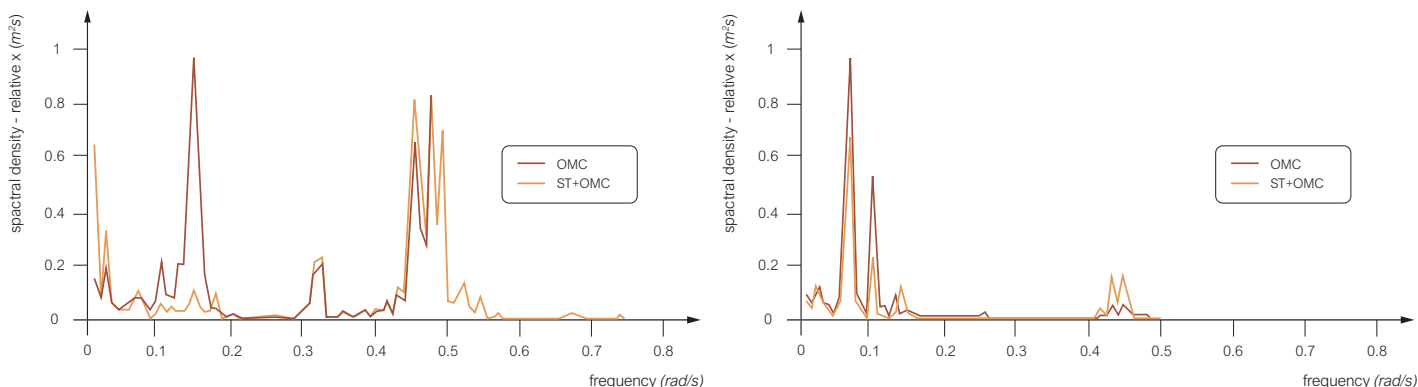


Figure 4.27: Spectral density of relative surge (top) and sway (bottom) (reworked from [Vreeburg, 2015](#), by TU Delft – Ports and Waterways is licenced under CC BY-NC-SA 4.0).

A [DMA](#) is executed to indicate possible problems due to (large) motions, and to evaluate the effectiveness of the measures that are considered to reduce these motions. For the ShoreTension example it can be seen that it is well capable of reducing the motions near the natural frequency, caused by low frequent excitation such as wind, long waves, or passing ships, but for other types of motions, other measures need to be considered in order to improve the workability.